Nonideality Consideration for High-Precision Amplifiers—Analysis of Random Common-Mode Rejection Ratio

Chong-Gun Yu and Randall L. Geiger, *Fellow, IEEE*

Abstract— **Nonideal factors which play a key role in performance and yield in high-precision applications of operational amplifiers are rigorously investigated. Of necessity, the combined effects of both deterministic and statistical parameters must be incorporated. The statistical characteristics of the common-mode rejection ratio and the offset of two-stage CMOS op-amps are investigated. The op-amp errors associated with finite open-loop gains, finite CMRR's, and nonzero offset voltages are analyzed. It is shown that the random common-mode gain as determined by the mismatch of paired devices is comparable to the deterministic common-mode gain. It is shown that the probability density function of the CMRR is distributed similar to that of a Gaussian random variable, but the mean is finite and the symmetry is skewed somewhat, as contrasted to the probability density function of the offset voltage which has a Gaussian distribution with zero mean. It is also shown that a nonideal finite CMRR can actually reduce the op-amp errors caused by a finite open-loop gain.**

List of Symbols

A	Open-loop gain for finite-CMRR and nonzero-offset op-amps
A'	Open-loop gain for finite-CMRR and zero-offset op-amps
A_c	Common-mode gain for nonzero-offset op-amps
A'_c	Common-mode gain for zero-offset op-amps
A_{cm}	Small signal common-mode voltage gain
A^D_{cm}	Deterministic common-mode gain
A^R_{cm}	Random common-mode gain
A_d	Open-loop gain for infinite-CMRR and nonzero-offset op-amps
A'_d	Open-loop gain for infinite-CMRR and zero-offset op-amps
A_{dm}	Small signal differential-mode voltage gain
β	Feedback factor of a closed-loop op-amp
$\boldsymbol{c}$	*CMRR* (a random variable)
C_{OX}	Oxide capacitance per unit area
$CMRR$	Common-mode rejection ratio
$CMRR'$	Common-mode rejection ratio for zero-offset op-amps
$CMRR_D^{-1}$	Reciprocal of the deterministic CMRR (defined as A^D_{cm}/A_{dm})
$CMRR_R^{-1}$	Reciprocal of the random CMRR (defined as A^R_{cm}/A_{dm})
d	$CMRR_D^{-1}$
E	Expected value
f	Probability density function
g_d	Output conductance
g_m	Transconductance gain
g_o	Output conductance of the bias current source
I_D	Drain current
K'	Transconductance coefficient defined as $\mu C_{OX}/2$
L	Channel length
λ	Channel length modulation parameter
μ	Bulk mobility
N	Normal (Gaussian) distribution
r	Absolute value of the ratio of d to σ_x
σ	Standard deviation
v_c, V_c	Common-mode input voltage
V_{CMRR}	Equivalent input voltage required for an infinite-CMRR op-amp
v_d, V_d	Differential-mode input voltage
V_{GS}	Gate-to-source voltage
V_i	Input voltage
v_o, V_o	Output voltage
V_{OS}	Input referred offset voltage
V_T	Threshold voltage
W	Channel width
$\boldsymbol{x}$	$CMRR_R^{-1}$ (a random variable)
$\boldsymbol{y}$	$\boldsymbol{x} + d$ (a random variable)

List of Subscripts

N	Nominal value
$R1$	Process dependent random variable, not varying from device to device on a wafer
$R2$	Wafer-level random variable, varying from device to device on a wafer
i	Input transistors (M1 and M2)
l	Load transistors (M3 and M4)

Manuscript received May 1, 1992; revised November 2, 1992. This paper was recommended by Associate Editor D. J. Allstot.

The authors are with the Department of Electrical and Computer Engineering, Iowa State University, Ames, IA 50011.

IEEE Log Number 9206241.

I. Introduction

NUMEROUS nonideal effects impact and generally degrade the performance of practical op-amps. Three factors—finite gain, finite common-mode rejection ratio (CMRR), and nonzero offset—are the major sources which limit the high-precision low-frequency applications of amplifiers. It is

well known that precision applications require a high open-loop gain, a large common-mode rejection ratio, and a low offset voltage, but practical limitations force the designer to make tradeoffs between these parameters. Because of the nonlinear relationship between these parameters and the performance parameters of interest, and because of the inherent statistical nature of the offset voltage and CMRR, the relationship between these parameters and the performance of amplifiers is still not fully formulated, causing designers to still commit nonoptimal designs to the foundry. For example, an infinite CMRR is often not optimal in the presence of a known finite open-loop gain of the op-amp. This paper focuses on a rigorous formulation of the relationship between these parameters and the performance of precision finite-gain amplifiers. Simple mathematically tractable relationships between the finite gain, CMRR, and offset voltage are developed and related to the overall performance of high-precision finite gain amplifiers. The CMRR and offset are not totally deterministic but have both deterministic and random components. Unfortunately, the performance and yield of systems using integrated op-amps are often dominated by the random components. These random components which are primarily due to the device mismatch make it difficult to analyze the op-amp errors. The statistical characteristics of these parameters must be well understood to practically obtain high-precision performance. Several analyses of the random offset [1], [2] and the random CMRR [5]–[7] in differential amplifiers have been made, but these analyses do not focus on the mixed effects of these nonidealities on amplifier performance. The analyses of the random CMRR [5]–[7], made several decades ago, concentrated only on bipolar differential amplifiers. Moreover, they focused on the methods to increase the CMRR, not on the statistical characteristics of this parameter which play a key role in the performance of precision finite gain amplifiers.

The impact of the CMRR may be best appreciated by reviewing the term itself. The term is widely used and has appeared in elementary electronics and instrumentation texts for many years [1]–[4]. For a single sample amplifier with differential input and single-ended output, the term is defined as

$$CMRR = \left| \frac{A_{dm}}{A_{cm}} \right| \tag{1}$$

where A_{dm} and A_{cm} are the small signal differential-mode and common-mode gains, respectively. Often it is expressed logarithmically rather than linearly. For the single sample amplifier, the CMRR is deterministic and can be readily measured in the laboratory. Of more important than the CMRR of a single sample amplifier from an operational amplifier yield viewpoint, from a discrete systems designers viewpoint, and from an integrated systems designers viewpoint, is the CMRR of an amplifier architecture in a process. In this case, the common-mode gain, which is ideally zero, becomes a key parameter in determining the CMRR. Since the common-mode gain invariably has a random component and a deterministic component, the same comment can be made about the CMRR.

Unfortunately, a rigorous definition of the CMRR has not appeared in the literature. Consequently, designers have been basing designs on inaccurate models and/or expensive "worst case" simulations where it is often difficult to ascertain that the simulations are actually worst case. The impact has often resulted in designs that are overly conservative or designs that have substantially degraded performance. The rigorous definition of the CMRR, although seemingly straightforward, is complicated by the observation that the CMRR is actually a random variable that is ideally infinite and that has a probability density function. The probability density function of the CMRR is nonlinearly related to the probability density functions of several other random variables which characterize the transistors comprising the operational amplifiers.

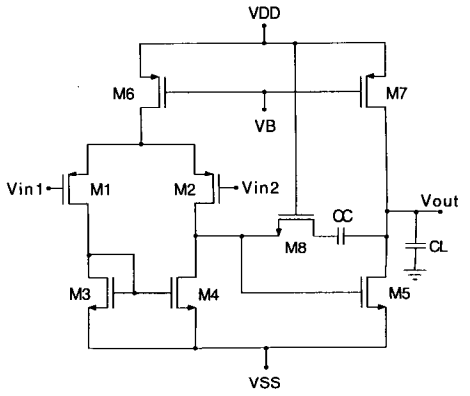

Fig. 1. Two-stage CMOS operational amplifier.

In this paper, the CMRR and offset of CMOS op-amps are thoroughly investigated. Op-amp induced errors in precision finite gain amplifiers due to these nonideal effects are compositely analyzed. A model amplifier of these analyses is the two-stage CMOS op-amp shown in Fig. 1. The sample op-amp has been designed for high-speed and high-precision applications in a 2μm CMOS process. The device sizes and other performance parameters are shown in Tables I and II. Although the formulations in this paper focus on the two-stage amplifier of Fig. 1, the results are readily extendable to other op-amp architectures as well.

II. Derivation of the Random and Deterministic CMRR

Since in multistage amplifiers the CMRR of the first stage is usually an important factor in the overall CMRR, the CMRR of the two-stage CMOS op-amp will be dominated by the first stage. The small signal equivalent circuit of the differential stage in Fig. 1 is shown in Fig. 2, where g_o denotes the internal output conductance of the transistor used as a bias current source. Ideally, M1 and M2 are matched as are M3 and M4.

The small-signal output voltage is given by

$$v_o = A_{dm}v_d + A_{cm}v_c \tag{2}$$

where

$$v_d = v_{in1} - v_{in2} \tag{3}$$

$$v_c = \frac{v_{in1} + v_{in2}}{2}. \tag{4}$$

The nodal equations at nodes (1), (2), and (3) are

$$\begin{aligned}(g_{m1} + g_{d1})v_1 - (g_{m3} + g_{d1})v_2 &= g_{m1}v_{in1} \\ (g_{m2} + g_{d2})v_1 - g_{m4}v_2 - (g_{d2} + g_{d4})v_{out} &= g_{m2}v_{in2}\end{aligned} \tag{5}$$

TABLE I
TRANSISTOR SIZE OF THE OP-AMP IN FIG. 1

Transistor	W/L (μ m/μ m)	Transistor	W/L (μ m/μ m)
M1	204/2	M2	204/2
M3	75/3	M4	75/3
M5	336/3	M6	100/2
M7	250/2	M8	14/4
V_B	3.3 V	C_C	2.39 pF

TABLE II
PERFORMANCE OF THE OP-AMP IN FIG. 1

Specification	Performance
Settling Time (1V Step, 0.1%)	18.3 nS
(2V Step, 5 mV)	16.5 nS
Systematic Input Offset Voltage	0.26 mV
Open Loop Voltage Gain	819.4 (58.27 dB)
Unit Gain Frequency (GB)	59 MHz
Phase Margin	75°
Output Voltage Swing	+4.1 V, −4.3 V
Power Dissipation	16.5 mW
CMRR	62.5 dB

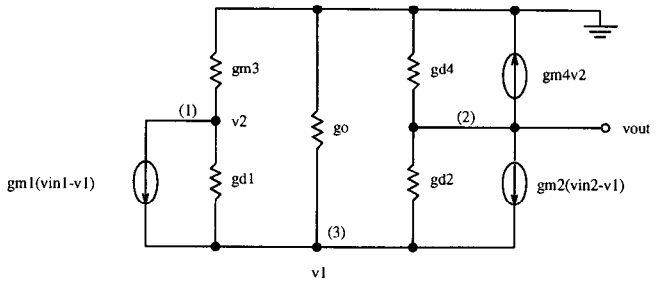

Fig. 2. Small signal equivalent circuit of the differential stage of Fig. 1.

$$(g_{m1}+g_{m2}+g_{d1}+g_{d2}+g_o)v_1 - g_{d1}v_2 - g_{d2}v_{out} = g_{m1}v_{in1}+g_{m2}v_{in2}.$$

The model parameters are all random variables and can be expressed as

$$\begin{aligned} g_{m1} &= g_{m1N}+g_{m1R1}+g_{m1R2} \\ g_{m2} &= g_{m2N}+g_{m2R1}+g_{m2R2} \\ g_{m3} &= g_{m3N}+g_{m3R1}+g_{m3R2} \\ g_{m4} &= g_{m4N}+g_{m4R1}+g_{m4R2} \\ g_{d1} &= g_{d1N}+g_{d1R1}+g_{d1R2} \\ g_{d2} &= g_{d2N}+g_{d2R1}+g_{d2R2} \\ g_{d4} &= g_{d4N}+g_{d4R1}+g_{d4R2}, \end{aligned} \tag{6}$$

where the N subscript denotes the nominal value which is deterministic, the $R1$ subscript denotes a random component that is process dependent but which does not vary from device to device on a wafer, and where the $R2$ subscript denotes a random component that varies randomly from device to device on a wafer. It will be assumed that process dependent random variables (those with an $R1$ subscript) are totally correlated and identical for matched devices and that the wafer-level random variables (those with an $R2$ subscript) are identically distributed for ideally matched devices but statistically uncorrelated.

Assuming that $g_{mk} \gg g_{dl}$, for all $k, l \in \{1, 2, 3, 4\}$, and that M1 and M2 are nominally matched as are M3 and M4, we can obtain the expressions for the differential-mode gain A_{dm} and the common-mode gain A_{cm}, which are themselves random variables (see (7) and (8), bottom of page), where

$$\begin{aligned} g_{mi} &= g_{m1N} = g_{m2N} \\ g_{miR1} &= g_{m1R1} = g_{m2R1} \\ g_{ml} &= g_{m3N} = g_{m4N} \\ g_{mlR1} &= g_{m3R1} = g_{m4R1} \\ g_{di} &= g_{d1N} = g_{d2N} \\ g_{diR1} &= g_{d1R1} = g_{d2R1} \\ g_{dl} &= g_{d4N}, \end{aligned} \tag{9}$$

where the i subscript denotes the input transistors M1 and M2, and the l subscript denotes the load transistors M3 and M4.

Since the random component of the differential gain is very small compared to the deterministic component of the differential gain as can be seen in (7), the total differential-mode gain can be approximated by the deterministic gain only. Hence,

$$\begin{aligned} A_{dm} &\simeq \frac{2g_{mi}^2 g_{ml}}{2g_{mi}g_{ml}(g_{di}+g_{dl})} \\ &= \frac{g_{mi}}{g_{di}+g_{dl}}. \end{aligned} \tag{10}$$

The random component of the common-mode gain is, however, comparable in magnitude to the deterministic component of the common-mode gain. The deterministic and random common-mode gains, A_{cm}^D and A_{cm}^R, can be defined so that

$$A_{cm} = A_{cm}^D + A_{cm}^R. \tag{11}$$

From (8), natural definitions of A_{cm}^D and A_{cm}^R are as shown in (12) and in (13) (see bottom of next page).

$$\begin{aligned} A_{cm}^D &= -\frac{g_{di}g_{mi}g_o}{2g_{mi}g_{ml}(g_{di}+g_{dl})} \\ &= -\frac{g_{di}g_o}{2g_{ml}(g_{di}+g_{dl})} \end{aligned} \tag{12}$$

$$A_{dm} \simeq \frac{2g_{mi}^2 g_{ml} + g_{mi}^2(2g_{mlR1}+g_{m3R2}+g_{m4R2}) + 2g_{mi}g_{ml}(2g_{miR1}+g_{m1R2}+g_{m2R2})}{2g_{mi}g_{ml}(g_{di}+g_{dl})} \tag{7}$$

$$A_{cm} \simeq \frac{-g_{di}g_{mi}g_o + (2g_{di}g_{ml}+g_o g_{ml})(g_{m1R2}-g_{m2R2}) - 2g_{mi}g_{ml}(g_{d1R2}-g_{d2R2}) - g_o g_{mi}(g_{m3R2}-g_{m4R2})}{2g_{mi}g_{ml}(g_{di}+g_{dl})}, \tag{8}$$

The ratios of the numerator of (13) are readily obtained in terms of the geometric and process device parameters. Details of this calculation appear in the Appendix. Substituting (84), (85), and (88) into (13) gives

$$A_{cm}^{R} = \frac{1}{2(g_{di}+g_{dl})}\left[g_o\left(\frac{W_{1R2}-W_{2R2}}{W_i} + \frac{L_{2R2}-L_{1R2}}{L_i} + \frac{W_{3R2}-W_{4R2}}{W_l} + \frac{L_{4R2}-L_{3R2}}{L_l} + \frac{V_{T2R2}-V_{T1R2}}{V_{GSi}-V_{Ti}} + \frac{V_{T4R2}-V_{T3R2}}{V_{GSl}-V_{Tl}}\right) + 2g_{di}\frac{V_{T1R2}-V_{T2R2}}{V_{GSi}-V_{Ti}}\right]. \quad (14)$$

The CMRR, defined in (1), where A_{cm} is now a random variable, is itself a random variable. If we define

$$CMRR_D^{-1} = \frac{A_{cm}^D}{A_{dm}} \quad (15)$$

$$CMRR_R^{-1} = \frac{A_{cm}^R}{A_{dm}}, \quad (16)$$

then we have

$$CMRR = \left|\frac{A_{dm}}{A_{cm}}\right| = \left|\frac{A_{dm}}{A_{cm}^D + A_{cm}^R}\right| = \left|\frac{1}{CMRR_D^{-1} + CMRR_R^{-1}}\right|. \quad (17)$$

From (10), (12), and (14)–(16), the deterministic and random CMRRs are given by

$$CMRR_D^{-1} = -\frac{g_{di}g_o}{2g_{mi}g_{ml}} \quad (18)$$

and

$$CMRR_R^{-1} = \frac{1}{2g_{mi}}\left[g_o\left(\frac{W_{1R2}-W_{2R2}}{W_i} + \frac{L_{2R2}-L_{1R2}}{L_i} + \frac{W_{3R2}-W_{4R2}}{W_l} + \frac{L_{4R2}-L_{3R2}}{L_l} + \frac{V_{T2R2}-V_{T1R2}}{V_{GSi}-V_{Ti}} + \frac{V_{T4R2}-V_{T3R2}}{V_{GSl}-V_{Tl}}\right) + 2g_{di}\frac{V_{T1R2}-V_{T2R2}}{V_{GSi}-V_{Ti}}\right]. \quad (19)$$

The deterministic CMRR given by (18) is as reported in [2] and [3]. From (19) we can see that the random component of the CMRR is caused by the nonzero output conductances of the bias current source and the input transistors as well as the mismatch of the paired devices. It can be seen that the effect due to g_o on the random CMRR is more dominant than that due to g_{di}.

TABLE III
SIMULATED PARAMETER VALUES OF THE OP- AMP IN FIG. 1

g_{mi}	1030 μA/V	g_{ml}	712 μA/V
g_o	43.7 μA/V	g_{di}	22.0 μA/V
$V_{GSi}-V_{Ti}$	0.393 V	$V_{GSl}-V_{Tl}$	0.542 V

We are accustomed to characterizing the CMRR by a single number. Unfortunately, it can be seen from (17)–(19) that the CMRR is actually a random variable and, as such, characterized by a probability density function, not a single number. Nonetheless, it is instructive to develop an appreciation for what the CMRR of sample amplifiers will be and to determine how important the random part of the CMRR actually is. At this stage, we will calculate a pseudo-worst case CMRR to compare the magnitude of the random and deterministic components of the CMRR. The probability density function itself will be explored in the next section.

To calculate the pseudo-worst case CMRR of the op-amp in Fig. 1, whose simulated parameter values are shown in Table III, it is assumed that the wafer-level random component of L and W are normally distributed with zero mean and standard deviation

$$\sigma_L = \sigma_W = 0.014\mu\text{m}. \quad (20)$$

We chose $\sigma_{\Delta L} = \sigma_{\Delta W} = 0.02\,\mu m$, which is a very reasonable choice as indicated in [10]. From the choice, (20) was obtained. Since $\Delta L = L_1 - L_2 = L_{1R2} - L_{2R2}$ and $\sigma_{\Delta L} = \sqrt{\sigma_{L1}^2 + \sigma_{L2}^2}, \sigma_L = \sigma_{L1} = \sigma_{L2} = \sigma_{\Delta L}/\sqrt{2} = 0.014\,\mu m$. It is also assumed that the corresponding random component of V_T is normally distributed with zero mean and standard deviation

$$\sigma_{V_T} = \frac{k}{\sqrt{LW}}, \quad (21)$$

where $k = 0.0236\,V\mu m$. The k value was obtained based on the choice of $\sigma_{\Delta V_T} = \frac{5}{3}$ mV for $LW = 20\times 20\,\mu m^2$ according to the experimental data in [11].

We define the pseudo-worst case CMRR to be the sample CMRR that would result if all random variables comprising the CMRR are in the direction that they add, and at the 3σ value that would most degrade the sample CMRR. The corresponding σ values for width, length, and threshold voltage variations are summarized in Table IV. The deterministic CMRR calculated from (18) was 63.7 dB, which is close to the simulated one shown in Table II. The pseudo-worst case random CMRR calculated from (19) was 51.6 dB which

$$A_{cm}^{R} = \frac{(2g_{di}g_{ml}+g_og_{ml})(g_{m1R2}-g_{m2R2}) - 2g_{mi}g_{ml}(g_{d1R2}-g_{d2R2}) - g_og_{mi}(g_{m3R2}-g_{m4R2})}{2g_{mi}g_{ml}(g_{di}+g_{dl})} = \frac{1}{2(g_{di}+g_{dl})}\left[g_o\left(\frac{g_{m1R2}-g_{m2R2}}{g_{mi}} - \frac{g_{m3R2}-g_{m4R2}}{g_{ml}}\right) + 2g_{di}\left(\frac{g_{m1R2}-g_{m2R2}}{g_{mi}} - \frac{g_{d1R2}-g_{d2R2}}{g_{di}}\right)\right]. \quad (13)$$

TABLE IV
COMPONENT σ VALUES FOR THE OP- AMP IN FIG. 1

σ_L	0.014 μm
σ_W	0.014 μm
$\sigma_{V_{Ti}}$	1.17 mV
$\sigma_{V_{Tl}}$	1.57 mV

dominates the deterministic CMRR. The worst case total CMRR was thus 49.6 dB. Since the random CMRR can have both positive and negative polarity, the total CMRR can be either improved or degraded by the random CMRR.

III. STATISTICAL CHARACTERISTICS OF CMRR

In this section, the statistical characteristics of the random variable, CMRR as defined by (17), will be investigated. For notational convenience we will define

$$\boldsymbol{c} = CMRR \tag{22}$$
$$\boldsymbol{x} = CMRR_R^{-1} \tag{23}$$
$$d = CMRR_D^{-1} \tag{24}$$
$$\boldsymbol{y} = \boldsymbol{x} + d \tag{25}$$

where the bold letters are used to denote random variables. From (17), the common-mode rejection ratio can be expressed as

$$\boldsymbol{c} = \left|\frac{1}{\boldsymbol{x}+d}\right| = \left|\frac{1}{\boldsymbol{y}}\right| = \frac{1}{|\boldsymbol{y}|}. \tag{26}$$

Equation (19) shows that the random variable $\boldsymbol{x} = CMRR_R^{-1}$ is a function of 12 random variables. These random variables are assumed to be independent and normally distributed with zero mean.

$$\begin{aligned} W_{1R2}, W_{2R2}, W_{3R2}, W_{4R2} &\sim N(0, \sigma_W^2) \\ L_{1R2}, L_{2R2}, L_{3R2}, L_{4R2} &\sim N(0, \sigma_L^2) \\ V_{T1R2}, V_{T2R2} &\sim N(0, \sigma_{V_{Ti}}^2) \\ V_{T3R2}, V_{T4R2} &\sim N(0, \sigma_{V_{Tl}}^2). \end{aligned} \tag{27}$$

Since $\boldsymbol{x}$ is the sum of 12 uncorrelated zero mean random variables, its mean will also be zero and its variance is equal to the sum of their variances. Thus, $\boldsymbol{x}$ is distributed as

$$\boldsymbol{x} \sim N(0, \sigma_x^2) \tag{28}$$

where

$$\sigma_x^2 = \frac{1}{2g_{mi}^2}\left[g_o^2\sigma_L^2\left(\frac{1}{L_i^2}+\frac{1}{L_l^2}\right) + g_o^2\sigma_W^2\left(\frac{1}{W_i^2}+\frac{1}{W_l^2}\right) + \frac{\sigma_{V_{Ti}}^2(g_o^2+4g_{di}^2)}{(V_{GSi}-V_{Ti})^2} + \frac{\sigma_{V_{Tl}}^2 g_o^2}{(V_{GSl}-V_{Tl})^2}\right]. \tag{29}$$

Since d in (24) is deterministic, the random variable $\boldsymbol{y} = \boldsymbol{x} + d$ is normally distributed with mean d and variance σ_x^2,

$$\boldsymbol{y} \sim N(d, \sigma_x^2). \tag{30}$$

The mean of $|\boldsymbol{y}|$ can be expressed as [8]

$$E\{|\boldsymbol{y}|\} = \sigma_x\sqrt{\frac{2}{\pi}}e^{-d^2/2\sigma_x^2} + 2dP\left(\frac{d}{\sigma_x}\right) - d \tag{31}$$

where

$$P(x) = \frac{1}{\sqrt{2\pi}}\int_{-\infty}^{x} e^{-y^2/2}\,dy. \tag{32}$$

The variance of $|\boldsymbol{y}|$ is then

$$\begin{aligned} \sigma_{|y|}^2 &= E\{|\boldsymbol{y}|^2\} - E^2\{|\boldsymbol{y}|\} \\ &= E\{\boldsymbol{y}^2\} - E^2\{|\boldsymbol{y}|\} \\ &= Var\{\boldsymbol{y}\} + E^2\{\boldsymbol{y}\} - E^2\{|\boldsymbol{y}|\} \\ &= \sigma_x^2 + d^2 - E^2\{|\boldsymbol{y}|\}. \end{aligned} \tag{33}$$

The probability density function, $f_c(c)$, of the common mode rejection ratio $\boldsymbol{c}$ can be obtained as follows. We want to determine the density of $\boldsymbol{c}$ in terms of the density of $\boldsymbol{y}$. Since $c > 0$, $f_c(c) = 0\,\forall c \le 0$. The equation $c = |\frac{1}{y}|$ has two solutions for $c > 0$,

$$y_1 = \frac{1}{c}, \qquad y_2 = -\frac{1}{c}. \tag{34}$$

From the fundamental theorem of determining the density of a function of a random variable [8], the pdf of $\boldsymbol{c}$ is then

$$\begin{aligned} f_c(c) &= \frac{f_y(y_1)}{|g'(y_1)|} + \frac{f_y(y_2)}{|g'(y_2)|} \\ &= \frac{1}{c^2}\left[f_y\left(\frac{1}{c}\right) + f_y\left(-\frac{1}{c}\right)\right], \end{aligned} \tag{35}$$

where $f_y(y)$ is the probability density function of $\boldsymbol{y}$, and $g(y) = |\frac{1}{y}|$. Since from (30) the pdf of $\boldsymbol{y}$ is

$$f_y(y) = \frac{1}{\sqrt{2\pi}\sigma_x}\exp\left[-\frac{(y-d)^2}{2\sigma_x^2}\right], \tag{36}$$

the pdf of the common-mode rejection ratio $\boldsymbol{c}$ becomes

$$f_c(c) = \frac{1}{\sqrt{2\pi}\sigma_x c^2}\left[\exp\left\{-\frac{(1-dc)^2}{2\sigma_x^2c^2}\right\} + \exp\left\{-\frac{(1+dc)^2}{2\sigma_x^2c^2}\right\}\right], \qquad c > 0. \tag{37}$$

The probability density curves of $\boldsymbol{c}$are shown in Fig. 3 where $r = |d/\sigma_x|$ and the $CMRR_D^{-1}$ of the op-amp in Fig. 1 was used for d. These curves show that the pdf of $\boldsymbol{c}$ is similar to a Gaussian density function, but it is not symmetric, and the left side of the peak point goes to zero faster than the right side, so the mean lies at the right of the peak point. Fig. 3 also shows that for the op-amp of Fig. 1, the CMRR probability below 55 dB is almost zero. Since the pdf of $\boldsymbol{c}$ is known, the mean and variance can be found from the expressions

$$E\{\boldsymbol{c}\} = \int_0^\infty c f_c(c)\,dc \tag{38}$$
$$\sigma_c^2 = E\{\boldsymbol{c}^2\} - E^2\{\boldsymbol{c}\}. \tag{39}$$

If $|\boldsymbol{y}|$ is concentrated near its mean, then $E\{\boldsymbol{c}\}$ and σ_c^2 can be approximated from the procedure of estimating the mean and variance of the functions of a random variable [8]. Let $\boldsymbol{c} = f(|\boldsymbol{y}|) = \frac{1}{|\boldsymbol{y}|}$ and $m = E\{|\boldsymbol{y}|\}$. If $f(|y|)$ is approximated by the first three terms of the Taylor series of $f(|y|)$ with center m, then

$$f(|y|) \simeq f(m) + f'(m)(|y| - m) + \frac{f''(m)}{2}(|y| - m)^2. \tag{40}$$

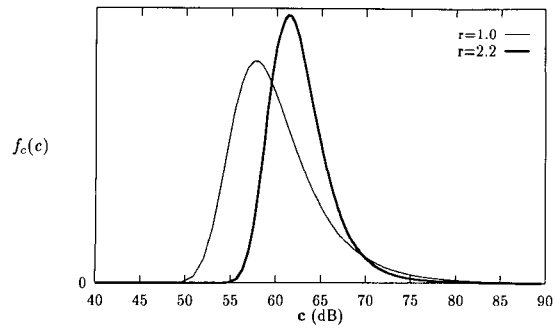

Fig. 3. Probability density curves of CMRR. $c = CMRR$ and $r = |d/\sigma_x|$.

Taking the expected values on (40), we obtain

$$E\{f(|\boldsymbol{y}|)\} \simeq f(m) + \frac{f''(m)}{2}(E\{|\boldsymbol{y}|^2\} - m^2). \tag{41}$$

The approximated $E\{\boldsymbol{c}\}$ is thus

$$E\{\boldsymbol{c}\} \simeq \frac{1}{E\{|\boldsymbol{y}|\}}\left[1 + \left(\frac{\sigma_{|y|}}{E\{|\boldsymbol{y}|\}}\right)^2\right]. \tag{42}$$

The first-order estimate of σ_c^2 is given by

$$\sigma_c^2 \simeq |f'(m)|^2\sigma_{|y|}^2 = \left(\frac{\sigma_{|y|}}{E^2\{|\boldsymbol{y}|\}}\right)^2. \tag{43}$$

The mean and variance of $|\boldsymbol{y}|$ are given in (31) and (33). From (37)–(39), (42), and (43) it is clear that the statistical characteristics of the common-mode rejection ratio, i.e., its mean, variance, and pdf, can be readily obtained if the variance of the process parameters are known.

The statistical parameters of the CMRR of the sample op-amp in Fig. 1 were calculated using the derived equations and the data in Tables III and IV. The approximated equations (42) and (43) were used to calculate $E\{\boldsymbol{c}\}$ and σ_c. The calculated results are listed in Column A of Table V. In order to investigate the correctness of these derived equations, 200 Gaussian random numbers with zero mean and variance σ_x^2 were generated and used to calculate the corresponding parameters. From these sample data of the random variable $\boldsymbol{x}$, the sample data of $|\boldsymbol{y}|$ and $\boldsymbol{c}$ can be obtained using (25) and (26). Their calculated mean and variance are shown in Column B of Table V. The $E\{|\boldsymbol{y}|\}$ and $\sigma_{|y|}$ from the derived equations are very close to those from the generated sample data, but the $E\{\boldsymbol{c}\}$ and σ_c of Column A somewhat differ from those of Column B because the $E\{\boldsymbol{c}\}$ and σ_c were calculated from the approximated equations (42) and (43). The histogram of the generated random data of $\boldsymbol{x}$ and the CMRR histogram are shown in Figs. 4 and 5. Since the $r(= |d/\sigma_x|)$ of the sample op-amp in Fig. 1 is 2.2, Fig. 5 corresponds to the curve ($r = 2.2$) of Fig. 3. These two plots are very similar and support the model of (37) for the pdf of $\boldsymbol{c}$.

IV. Definition of the CMRR for Processes

The random offset of a CMOS amplifier has been defined for processes as three times its standard deviation. The reason is that the offset voltage has a Gaussian distribution, so 99.7% of a sample satisfies the specification. Attention, however, has not been paid to the random CMRR of CMOS amplifiers, and no definition of the CMRR including random components has been made. Thus, the CMRR of CMOS op-amps for processes will be defined in this section.

In the previous section we found the probability density function $f_c(c)$ of the CMRR. We will define the CMRR to the value of $\hat{c}$ such that 99.86% of a sample set has a CMRR greater than $\hat{c}$. The choice of the 99.86%, which is close to the 99.7% used in the definition of offset voltages discussed above, will be discussed later. Integration of the pdf, $f_c(c)$, from $\hat{c}$ to infinity gives the following results:

$$\int_{\hat{c}}^{\infty} f_c(c)\,dc = P(a) + P(b) - 1 \tag{44}$$

TABLE V
The CMRR Statistical Characteristics of the Op-Amp in Fig. 1b Calculated (A) From the Derived Equations and (B) from the 200 Generated Random Numbers

	A	B
d	-6.55×10^{-4}	
σ_x	2.976×10^{-4}	2.763×10^{-4}
$E\{\lvert\boldsymbol{y}\rvert\}$	6.579×10^{-4}	6.612×10^{-4}
$\sigma_{\lvert y\rvert}$	2.797×10^{-4}	2.691×10^{-4}
$E\{\boldsymbol{c}\}$	1.795×10^{3} (65 dB)	2.017×10^{3} (66 dB)
σ_c	6.462×10^{2}	1.847×10^{3}

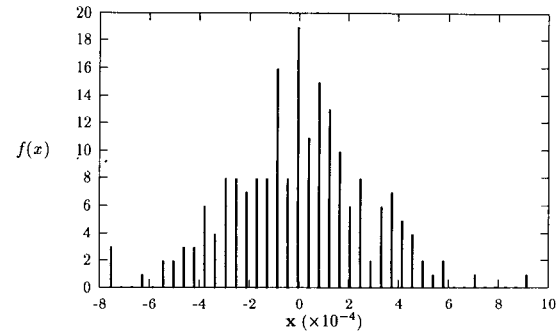

Fig. 4. Histogram of the 200 samples generated for the random variable $\boldsymbol{x}$. $\boldsymbol{x} = CMRR_R^{-1}$.

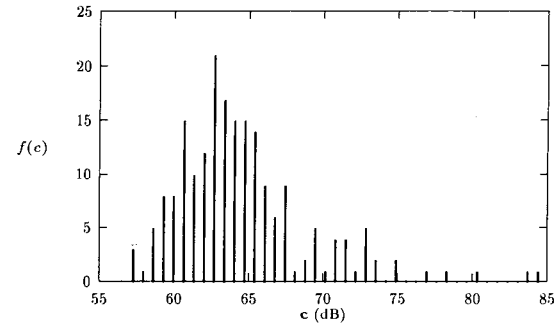

Fig. 5. Histogram of the 200 samples calculated from the data in Fig. 4 for the random variable $\boldsymbol{c}$. $\boldsymbol{c} = CMRR$.

where

$$a = \frac{1/\hat{c} - d}{\sigma_x} \tag{45}$$

$$b = \frac{1/\hat{c} + d}{\sigma_x} \tag{46}$$

Since d is negative for the sample op-amp, we can rewrite a and b as

$$a = \frac{1}{\sigma_x \hat{c}} + \left|\frac{d}{\sigma_x}\right|, \qquad b = \frac{1}{\sigma_x \hat{c}} - \left|\frac{d}{\sigma_x}\right|. \tag{47}$$

From (47) we can see that a is always greater than b by $2|d/\sigma_x|$. Thus, $P(a)$ is also always greater than $P(b)$ because $P(x)$ defined in (32) increases from 0.5 to 1.0 as x increases from 0 to ∞.

Since we want to make

$$\int_{\hat{c}}^{\infty} f_c(c)\, dc = 0.9986, \tag{48}$$

$P(b)$ should be very close to 1.0. This means that $P(a)$ is almost 1.0 because $P(a)$ is greater than $P(b)$, and the maximum value of the function $P(x)$ is 1.0. In most cases, $|d/\sigma_x| > 0.5$, so $a > b + 1$. Therefore, under the condition of (48), the approximation

$$\int_{\hat{c}}^{\infty} f_c(c)\, dc \simeq P(b) = P\left(\frac{1/\hat{c} + d}{\sigma_x}\right) \tag{49}$$

can be used. From (48) and (49) we obtain

$$P\left(\frac{1/\hat{c} + d}{\sigma_x}\right) = 0.9986. \tag{50}$$

It now follows from tables for $P(x)$ [9] that (50) will be satisfied provided

$$\frac{1/\hat{c} + d}{\sigma_x} = 3 \tag{51}$$

which can be expressed as

$$\hat{c} = (3\sigma_x - d)^{-1}. \tag{52}$$

The reason we chose a figure of 0.9986 in (48) was to obtain the integer 3 in (51). If we use $(3\sigma_x - d)^{-1}$ as the CMRR specification in designing CMOS amplifiers, then 99.86% of a large sample will satisfy the specification. If d is positive, then $P(b)$ is greater than $P(a)$, and finally we have

$$\hat{c} = (3\sigma_x + d)^{-1}. \tag{53}$$

Therefore, we can define the CMRR for processes as

$$CMRR = (3\sigma_x + |d|)^{-1} \tag{54}$$

where d and σ_x are $CMRR_D^{-1}$ and the standard deviation of $CMRR_R^{-1}$. The $CMRR_D^{-1}$ and $CMRR_R^{-1}$ were defined in (15) and (16). The calculated CMRR for the sample op-amp in Fig. 1 was 56.2 dB. Comparing with the density curve ($r = 2.2$) in Fig. 3, we can see that the value 56.2 dB is very reasonable.

The CMRR definition for processes of (54) and the CMRR pdf of (37) are general for the op-amps whose deterministic and random components comparably contribute to the total CMRR. This case usually corresponds to the op-amps whose first stage has a single-ended output. If op-amps have a first stage with differential output, then their deterministic common-mode gains are significantly reduced by the next stages [6]. In these cases, the deterministic CMRR can be ignored, i.e., $d \simeq 0$, and the above CMRR definition and the pdf should be changed. If d is nearly zero, then the pdf of the total CMRR is

$$f_c(c) = \frac{2}{\sqrt{2\pi}\sigma_x c^2} \exp\left[-\frac{1}{2\sigma_x^2 c^2}\right], \qquad c > 0. \tag{55}$$

The integration of the pdf from $\hat{c}$ to ∞ becomes

$$\int_{\hat{c}}^{\infty} f_c(c)\, dc = 2P\left(\frac{1}{\sigma_x \hat{c}}\right) - 1. \tag{56}$$

The CMRR definition for processes is thus

$$CMRR = (3\sigma_x)^{-1} \tag{57}$$

where 99.73% of a sample set will be greater than $(3\sigma_x)^{-1}$. The approximated mean and variance of the CMRR have the same equations (42) and (43), but the $E\{|\boldsymbol{y}|\}$ and $\sigma_{|\boldsymbol{y}|}$ should be modified as follows:

$$E\{|\boldsymbol{y}|\} = \sigma_x \sqrt{\frac{2}{\pi}} \tag{58}$$

$$\sigma_{|\boldsymbol{y}|} = \sigma_x^2 \left(1 - \frac{2}{\pi}\right). \tag{59}$$

V. Offset Analysis

The offset voltage of an op-amp consists of two components: a deterministic offset and a random offset. The former results from improper dimensions and/or bias conditions, so it can be reduced to a very small value by careful design. The latter is due to the random errors in the fabrication process, i.e., mismatches in identically designed pairs of devices. For two-stage op-amps, the first stage will have a dominant effect on the offset. Therefore, the total input referred offset voltage of the two-stage op-amp will be highly affected by the first-stage random offset voltage. The input offset voltage, V_{OS}, is defined as the differential input voltage that is required to make the differential output voltage exactly zero. If both input terminals are grounded, then the input referred offset voltage of the first stage can be expressed as

$$\begin{aligned} V_{OS} &= \frac{V_o}{A} \\ &= \frac{\Delta I_D}{g_m} \\ &= \frac{\Delta I_D}{2I_D/(V_{GSi} - V_{Ti})} \\ &= \frac{V_{GSi} - V_{Ti}}{2} \frac{\Delta I_D}{I_D}, \end{aligned} \tag{60}$$

where V_o is the first-stage output voltage, and A is the first-stage small-signal voltage gain.

Since ΔI_D is mainly affected by the mismatch in the threshold voltage and the device width and length, and other factors can be ignored [10], we will consider only offsets

in the V_T and W/L of the input differential pair (M1 and M2) and the current mirror pair (M3 and M4) in Fig. 1. The $\Delta I_{Di} = I_{D1} - I_{D2}$ due to the mismatch of the input differential pair and the $\Delta I_{Dl} = I_{D3} - I_{D4}$ due to the mismatch of the current mirror pair are given from the Appendix. Substituting (89) and (90) into (60), we have the input offset voltage due to the mismatch of the input differential pair,

$$V_{OSi} = V_{T2R2} - V_{T1R2} + \frac{V_{GSi} - V_{Ti}}{2} \cdot \left(\frac{W_{1R2} - W_{2R2}}{W_i} + \frac{L_{2R2} - L_{1R2}}{L_i} \right), \quad (61)$$

and the input offset voltage due to the current mirror pair,

$$V_{OSl} = \frac{V_{GSi} - V_{Ti}}{2} \left(\frac{W_{3R2} - W_{4R2}}{W_l} + \frac{L_{4R2} - L_{3R2}}{L_l} \right) + \frac{V_{GSi} - V_{Ti}}{V_{GSl} - V_{Tl}} (V_{T4R2} - V_{T3R2}). \quad (62)$$

The total input referred offset with be the sum of these terms (61) and (62),

$$\begin{aligned} V_{OS} &= V_{OSi} + V_{OSl} \\ &= \frac{V_{GSi} - V_{Ti}}{2} \left[\frac{W_{1R2} - W_{2R2}}{W_i} + \frac{L_{2R2} - L_{1R2}}{L_i} \right. \\ &\quad + \frac{W_{3R2} - W_{4R2}}{W_l} + \frac{L_{4R2} - L_{3R2}}{L_l} \\ &\quad \left. + \frac{2(V_{T2R2} - V_{T1R2})}{V_{GSi} - V_{Ti}} + \frac{2(V_{T4R2} - V_{T3R2})}{V_{GSl} - V_{Tl}} \right]. \end{aligned} \quad (63)$$

Since the offset voltage is the sum of 12 uncorrelated zero mean Gaussian random variables, it is also normally distributed with zero mean and standard deviation

$$\sigma_{V_{OS}} = \frac{(V_{GSi} - V_{Ti})}{\sqrt{2}} \left[\sigma_L^2 \left(\frac{1}{L_i^2} + \frac{1}{L_l^2} \right) + \sigma_W^2 \left(\frac{1}{W_i^2} + \frac{1}{W_l^2} \right) + \frac{4\sigma^2_{V_{Ti}/}}{(V_{GSi} - V_{Ti})^2} + \frac{4\sigma^2_{V_{Tl}}}{(V_{GSl} - V_{Tl})^2} \right]^{\frac{1}{2}}. \quad (64)$$

Therefore, the offset has a Gaussian density function with zero mean and variance $\sigma_{V_{OS}}$.

Assuming again the pseudo-worst case as in Section II, and using the data of Tables III and IV, the calculated pseudo-worst case random offset of the sample op-amp in Fig. 1 is 27.9 mV. The offset due to the (W/L) mismatch is 14.1 mV while the offset due to the V_T mismatch is 13.8 mV. It shows that the two factors give almost equal contribution to the random offset for the sample op-amp.

VI. Analysis of Op-Amp Errors

The gain of a unity-gain configured op-amp will be exactly one if the op-amp is ideal. Practical op-amps, however, don't offer the exact gain because of finite differential gains, finite common-mode rejection ratios, and nonzero offset voltages. In this section, the op-amp errors associated with these nonideal effects are analyzed. First, we define the different open-loop gains as shown in Fig. 7. We denote the finite open-loop gains of the op-amps which have different characteristics as follows:

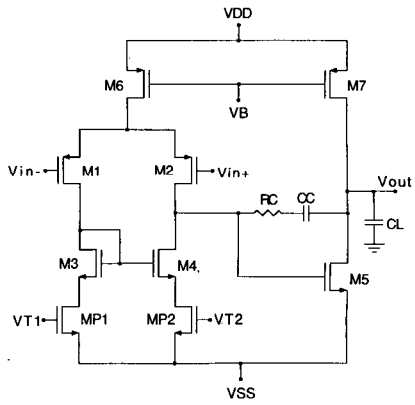

Fig. 6. Two-stage CMOS operational amplifier with a programmable current mirror.

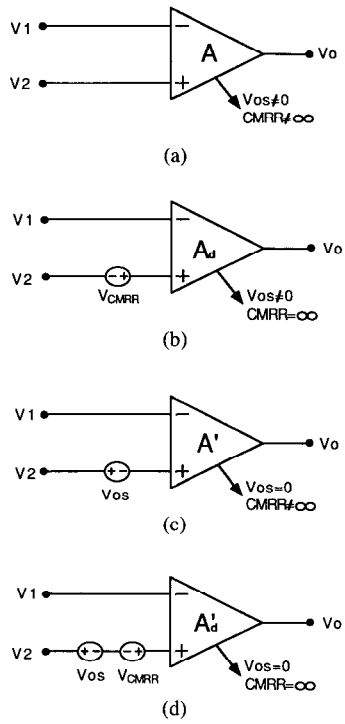

Fig. 7. Equivalent models for a nonideal op-amp interpreting CMRR and offset and showing differently defined open-loop gains.

A:	Finite CMRR and nonzero offset
A_d:	Infinite CMRR and nonzero offset
A':	Finite CMRR and zero offset
A'_d:	Infinite CMRR and zero offset.

Simulated results of these gains for the op-amp in Fig. 6 obtained by neglecting statistical variations are shown in Table VI, where $A_c, CMRR, A'_c$, and $CMRR'$ are the common mode gains and the common mode rejection ratios of a nonzero offset op-amp and a zero offset op-amp, respectively. The V_{OS} is the input referred offset voltage. The op-amp in Fig. 6 differs from that in Fig. 1. It has a programmable current mirror

TABLE VI
SIMULATED GAINS OF THE OP-AMP IN FIG.6

A	386.8	A'	386.6
A_d	386.5	A'_d	386.2
A_c	0.4811	A'_c	0.4803
$CMRR$	805.8	$CMRR'$	805.8
V_{OS}	-20.4 μV		

instead of a simple one as a load of the differential input pair. The programmable current mirror can be used to compensate the offset voltage of the op-amp by adjusting the bias voltages VT1 and/or VT2 as described in [12] and [13]. Basic concepts concerning the influence of each nonideal factor are briefly reviewed in the following three subsections. This is followed by discussions about the combined effects of the nonideal factors.

A. Finite Open-Loop Gain Effect

Assuming that an op-amp has an infinite CMRR and a zero offset, the output voltage of the unity-gain configured op-amp will be

$$V_o = \frac{A'_d}{1 + A'_d} V_i. \tag{65}$$

If the pure differential gain A'_d is infinity, then the input V_i will be equal to the output V_o, but the output of a practical op-amp will be less than the input due to the finite open-loop gain. Hence, the gain of a unity-gain configured op-amp will always be less than one under the assumption of infinite CMRR and zero offset.

B. Finite CMRR Effect

Considering a finite-CMRR and zero-offset op-amp which is equivalent to the op-amp in Fig. 7(c) if the voltage source V_{OS} is removed, the output of the op-amp will consist of two terms:

$$\begin{aligned} V_o &= V_c A'_c + V_d A'_d \\ &= \frac{V_1 + V_2}{2} A'_c + (V_2 - V_1) A'_d \\ &= \frac{V_1 + V_2}{2CMRR'} A'_d + (V_2 - V_1) A'_d. \end{aligned} \tag{66}$$

From these equations, the op-amp can be modeled as in Fig. 7(d) if the voltage source V_{OS} in Fig. 7(d) is removed, where

$$V_{CMRR} = \frac{V_1 + V_2}{2CMRR'}. \tag{67}$$

If this op-amp is used for a unity-gain configuration, i.e., $V_1 = V_o$ and $V_2 = V_i$, then the output voltage will be

$$\begin{aligned} V_o &= A'_d(V_i + V_{CMRR'} - V_o) \\ &= A'_d\left(V_i + \frac{V_i + V_o}{2CMRR'} - V_o\right). \end{aligned} \tag{68}$$

Hence,

$$V_o = \frac{A'_d\left(1 + \frac{1}{2CMRR'}\right)}{A'_d\left(1 - \frac{1}{2CMRR'}\right) + 1} V_i. \tag{69}$$

It can be seen that an infinite CMRR reduces (69) to (65). Equation (69) shows that the finite CMRR can compensate or overcompensate for the gain decreasing effect due to the finite open-loop gain.

C. Nonzero Offset Effect

To investigate the effect of nonzero offset, we consider an nonzero-offset and infinite-CMRR which is equivalent to the op-amp in Fig. 7(b) if the voltage source V_{CMRR} is removed. The input referred offset voltage can be defined as the voltage applied at the positive input so that the voltage existing at the output becomes zero. Thus, the nonzero-offset and infinite-CMRR op-amp can be modeled as a voltage source V_{OS} which is equivalent to the input offset voltage and a pure differential op-amp. This model is equivalent to Fig. 7(d) if the voltage source V_{CMRR} is removed. If this op-amp is used for a unity-gain configuration, then the output voltage will be

$$V_o = A'_d(V_i - V_{OS} - V_o). \tag{70}$$

Hence,

$$V_o = \frac{A'_d}{1 + A'_d}(V_i - V_{OS}), \tag{71}$$

where it is well known that the offset voltage can be either positive or negative.

D. Total Op-Amp Error

Now, the three effects are combined to derive the total op-amp error. The nonideal op-amp shown in Fig. 7(a) can be modeled as two voltage sources, V_{OS} and V_{CMRR}, applied at the positive input and a pure differential op-amp which has an infinite CMRR and a zero offset voltage as shown in Fig. 7(d). The output is then

$$\begin{aligned} V_o &= A'_d(V_2 - V_{OS} + V_{CMRR} - V_1) \\ &= A'_2\left(V_2 - V_{OS} + \frac{V_1 + V_2 - V_{OS}}{2CMRR'} - V_1\right). \end{aligned} \tag{72}$$

If this op-amp is used for a unity-gain configuration as shown in Fig. 8(a), then the output will be

$$V_o = A'_d\left(V_i - V_{OS} + \frac{V_o + V_i - V_{OS}}{2CMRR'} - V_o\right). \tag{73}$$

The total output affected by a finite gain, a finite CMRR, and a nonzero offset is thus given by

$$V_o = \frac{A'_d\left(1 + \frac{1}{2CMRR'}\right)}{A'_d\left(1 - \frac{1}{2CMRR'}\right) + 1}(V_i - V_{OS}) \tag{74}$$

where

$$CMRR' = \frac{A'_d}{A'_c} \approx \frac{A_d}{A_c} = CMRR. \tag{75}$$

If the op-amp is used for a high-gain configuration as shown in Fig. 8(b), then the output becomes

$$V_o = \frac{A'_d\left(1 + \frac{1}{2CMRR'}\right)}{A'_d\beta\left(1 - \frac{1}{2CMRR'}\right) + 1}(V_i - V_{OS}) \tag{76}$$

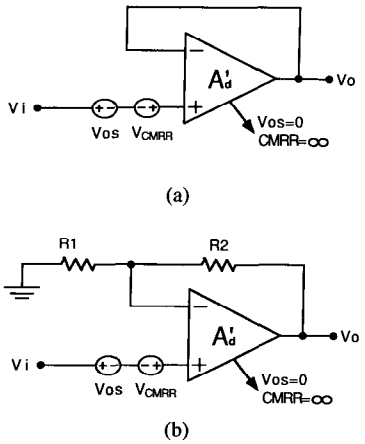

Fig. 8. (a) Model of a unity-gain configured op-amp, and (b) model of a high-gain configured op-amp.

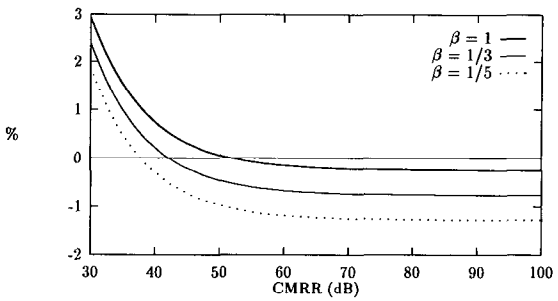

Fig. 9. Output error of the op-amp in Fig. 6 versus CMRR with β as a parameter. The offset voltage $V_{OS} = 0$, and the open-loop gain $A = 52$ dB.

where

$$\beta = \frac{R_1}{R_1 + R_2}. \tag{77}$$

From (74), it can be easily seen that (71), (69), and (65) can be obtained by setting $V_{OS} = 0, CMRR' = \infty$, and both of them, respectively.

From (74) and the data given in Table VI, the calculated unity-gain configured output voltage of the op-amp in Fig. 6 is 0.9987 V when $V_i = 1.0$ V, while the simulated settling point of the output voltage is 0.9988 V. This result shows that (74) gives a very consistent result with the simulated one. In this example, the random CMRR and the random offset have not been considered, but the correctness of (74) has been demonstrated. In practical op-amps, that kind of accuracy could not be obtained because of the random components described in the previous sections. With the assumption that $V_{OS} = 0$, the output errors of the op-amp in Fig. 6 as a function of CMRR were calculated at different closed-loop gains, and the results are shown in Fig. 9. Even though the offset is zero and the CMRR is very high, the output error of the unity-gain configured op-amp ($\beta = 1$) is about 0.3% due to the finite open-loop gain. If the CMRR is 52 dB, then the output error is nearly zero. This shows that the finite CMRR can reduce the error attributable to the finite gain as mentioned in Section VI-B. From the figure it can also be seen that high-gain configured op-amps show more errors than low-gain op-amps.

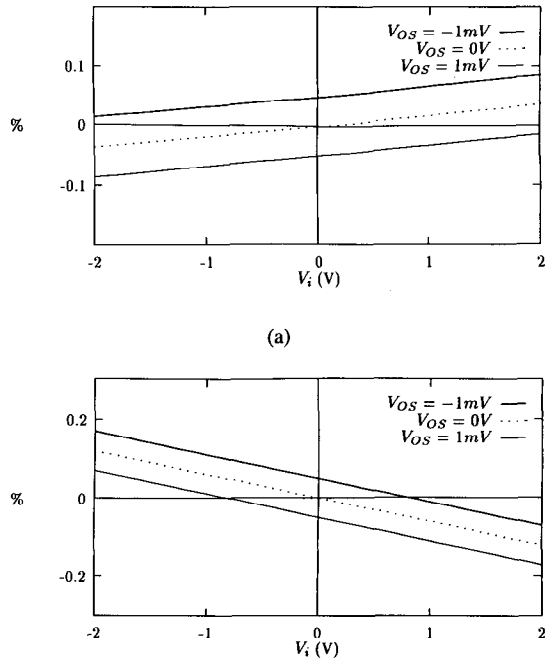

Fig. 10. Output error of the op-amp in Fig. 1 versus V_i and V_{OS} as a parameter. The open-loop gain $A = 58\,dB$, and CMRR's are: (a) 56 dB and (b) 100 dB.

If the offset of a given op-amp is compensated, and the compensated offset range is known, then the output error of the given op-amp can be analyzed from (74) and (76) because the CMRR range of the op-amp can be easily found from the pdf of the CMRR derived in Section III or the CMRR definition in Section IV. Assuming that the offset is adjusted to less than 1 mV in magnitude, the output errors of the sample op-amp in Fig. 1 were analyzed. It was shown in Section IV that the sample op-amp in Fig. 1 had CMRR for the process of about 56 dB. Thus, the CMRR of most individual amplifiers will be greater than 56 dB. Fig. 10 shows the output errors relative to 2 V of the unity-gain configured sample op-amp as a function of the input V_i. From the 56 dB CMRR curves in Fig. 10(a) and the 100 dB CMRR curves in Fig. 10(b), it can be seen that the output errors are less than 0.2% through the input range of -2 V to +2 V if the magnitude of the input offset is less than 1 mV. As expected, the 56 dB CMRR curves show reduced errors compared to those of the 100 dB CMRR curves.

VII. Conclusions

The CMRR and offset of two-stage CMOS op-amps have been analyzed. Equations representing their statistical characteristics have been derived. Using these equations, we can readily find the distribution, mean, and variance of the CMRR and offset if the process parameter variations are given. The derived equations have shown that the CMRR pdf is similar to that of a Gaussian random variable, but the mean is not zero and the symmetry is somewhat skewed, whereas the offset has a Gaussian distribution with zero mean. The CMRR for the processes has been defined. The CMRR is defined by $(3\sigma_x + |d|)^{-1}$ for the op-amps which have both dominant

deterministic and random CMRR so that 99.86% of a large sample can be greater than the defined value. For the op-amps whose deterministic CMRR's are nearly zero, $(3\sigma_x)^{-1}$ can be used for the definition of the CMRR, where 99.73% of a large sample satisfies the specification. The variable d is the ratio of the deterministic common-mode gain to the differential-mode gain, and σ_x is the standard deviation of the ratio of the random common-mode gain to the differential-mode gain.

The op-amp errors due to finite open-loop gains, finite CMRR's, and nonzero offsets have been analyzed. A finite differential open-loop gain always makes the gain of a unity-gain configured op-amp less than one, and a finite CMRR can compensate for the error attributable to the finite open-loop gain unless it is too small. If the compensated offset range is known, then the op-amp error range can be found.

VIII. Appendix

If the channel-length modulation effect is ignored, the small-signal transconductance gains of the paired transistors M1 and M2 which act in the saturation region are given by

$$g_{m1} = 2K'\left(\frac{W}{L}\right)_1 (V_{GSi} - V_{T1}) \tag{78}$$

$$g_{m2} = 2K'\left(\frac{W}{L}\right)_2 (V_{GSi} - V_{T2}), \tag{79}$$

where $K' = \mu C_{OX}/2$. Only mismatches in the V_T and W/L are considered. The similar expressions as in (6) for the random variables, L, W, and V_T, can be used as follows:

$$L_1 = L_i + L_{iR1} + L_{1R2}, \quad L_2 = L_i + L_{iR1} + L_{2R2}$$

$$W_1 = W_i + W_{iR1} + W_{1R2}, \quad W_2 = W_i + W_{iR1} + W_{2R2}$$

$$V_{T1} = V_{Ti} + V_{TiR1} + V_{T1R2}, \quad V_{T2} = V_{Ti} + V_{TiR1} + V_{T2R2}, \tag{80}$$

where L_i, W_i, and V_{Ti} are the nominal values, and the subscripts $R1$ and $R2$ are the same as before.

Using these definitions, g_{m1} can be approximated by ignoring higher order terms,

$$\begin{aligned} g_{m1} &= 2K'\left(\frac{W_i + W_{iR1} + W_{1R2}}{L_i + L_{iR1} + L_{1R2}}\right) \\ &\quad \times (V_{GSi} - V_{Ti} - V_{TiR1} - V_{T1R2}) \\ &= 2K'\left(\frac{W_i}{L_i}\right)(V_{GSi} - V_{Ti})\left(\frac{1 + (W_{iR1} + W_{1R2})/W_i}{1 + (L_{iR1} + L_{1R2})/L_i}\right) \\ &\quad \cdot \left(1 - \frac{V_{TiR1} + V_{T1R2}}{V_{GSi} - V_{Ti}}\right) \\ &\simeq g_{mi}\left(1 + \frac{W_{iR1} + W_{1R2}}{W_i}\right)\left(1 - \frac{L_{iR1} + L_{1R2}}{L_i}\right) \\ &\quad \cdot \left(1 - \frac{V_{TiR1} + V_{T1R2}}{V_{GSi} - V_{Ti}}\right) \\ &\simeq g_{mi}\left(1 + \frac{W_{iR1} + W_{1R2}}{W_i} - \frac{L_{iR1} + L_{1R2}}{L_i} \right. \\ &\quad \left. - \frac{V_{TiR1} + V_{T1R2}}{V_{GSi} - V_{Ti}}\right). \end{aligned} \tag{81}$$

By the same way,

$$g_{m2} \simeq g_{mi}\left(1 + \frac{W_{iR1} + W_{2R2}}{W_i} - \frac{L_{iR1} + L_{2R2}}{L_i} - \frac{V_{TiR1} + V_{T2R2}}{V_{GSi} - V_{Ti}}\right). \tag{82}$$

Hence,

$$g_{m1} - g_{m2} = g_{mi}\left(\frac{W_{1R2} - W_{2R2}}{W_i} + \frac{L_{2R2} - L_{1R2}}{L_i} - \frac{V_{T2R2} - V_{T1R2}}{V_{GSi} - V_{Ti}}\right). \tag{83}$$

Since $g_{m1} - g_{m2} = g_{m1R2} - g_{m2R2}$ from (6) and (9),

$$\frac{g_{m1R2} - g_{m2R2}}{g_{mi}} = \frac{W_{1R2} - W_{2R2}}{W_i} + \frac{L_{2R2} - L_{1R2}}{L_i} + \frac{V_{T2R2} - V_{T1R2}}{V_{GSi} - V_{Ti}}. \tag{84}$$

By the same procedure,

$$\frac{g_{m3R2} - g_{m4R2}}{g_{ml}} = \frac{W_{3R2} - W_{4R2}}{W_l} + \frac{L_{4R2} - L_{3R2}}{L_l} + \frac{V_{T4R2} - V_{T3R2}}{V_{GSl} - V_{Tl}}. \tag{85}$$

Since the drain current I_D and the output conductance g_d can be expressed as

$$I_D = K'\left(\frac{W}{L}\right)(V_{GS} - V_T)^2 \tag{86}$$

$$g = \lambda I_D, \tag{87}$$

by the same method as above we can obtain

$$\frac{g_{d1R2} - g_{d2R2}}{g_{di}} = \frac{W_{1R2} - W_{2R2}}{W_i} + \frac{L_{2R2} - L_{1R2}}{L_i} + \frac{2(V_{T2R2} - V_{T1R2})}{V_{GSi} - V_{Ti}}, \tag{88}$$

and

$$\frac{I_{D1} - I_{D2}}{I_{Di}} = \frac{W_{1R2} - W_{2R2}}{W_i} + \frac{L_{2R2} - L_{1R2}}{L_i} + \frac{2(V_{T2R2} - V_{T1R2})}{V_{GSi} - V_{Ti}} \tag{89}$$

$$\frac{I_{D3} - I_{D4}}{I_{Dl}} = \frac{W_{3R2} - W_{4R2}}{W_l} + \frac{L_{4R2} - L_{3R2}}{L_l} + \frac{2(V_{T4R2} - V_{T3R2})}{V_{GSl} - V_{Tl}} \tag{90}$$

where $I_D = I_{Di} = I_{Dl}$.

Acknowledgment

The authors would like to thank Prof. T. M. Scott and Prof. S. G. Burns of Iowa State University, Ames, for their valuable discussions and comments.

REFERENCES

[1] P. R. Gray and R. G. Meyer, *Analysis and Design of Analog Integrated Circuits*. New York: Wiley, 1984.

[2] R. Gregorian and G. C. Temes, *Analog MOS Integrated Circuits For Signal Processing*. New York: Wiley, 1986.

[3] R. Unbehauen and A. Cichocki, *MOS Switched-Capacitor and Continuous-Time Integrated Circuits and Systems*. New York: Springer-Verlag, 1989.

[4] R. L. Geiger, P. E. Allen, and N. R. Strader, *VLSI Design Techniques for Analog and Digital Circuits*. New York: McGraw-Hill, 1990.

[5] J. I. Brown, "Differential amplifiers that reject common-mode currents," *IEEE J. Solid-State Circuits*, vol. SC-6, pp. 385–391, Dec. 1971.

[6] G. Meyer-Brotz and A. Kley, "The common-mode rejection of transistor differential amplifiers," *IEEE Trans. Circuits Theory*, vol. CT-13, pp. 171–175, June 1966.

[7] P. M. Vanpeterghem and J. F. Duque-Carrillo, "A general description of common-mode feedback in fully-differential amplifiers," in *Proc. IEEE Int. Symp. CAS*, 1990, pp. 3209–3212.

[8] A. Papoulis, *Probability, Random Variables, and Stochastic Processes*. New York: McGraw-Hill, 1984.

[9] M. Abramowitz and I. E. Stegun, *Handbook of Mathematical Functions with Formulas, Graphs, and Mathematical Tables*, National Bureau of Standards, AMS 55, Dec. 1972.

[10] K. R. Lakshmikumar, R. A. Hadaway, and M. A. Copeland, "Characterization and modeling of mismatch in MOS transistors for precision analog design," *IEEE J. Solid-State Circuits*, vol. SC-21, pp. 1057–1066, Dec. 1986.

[11] M. J. Pelgram, A. C. Duinmaijer, and A. P. Welbers, "Matching properties of MOS transistors," *IEEE J. Solid-State Circuits*, vol. 24, pp. 1433–1439, Oct. 1989.

[12] M. Degrauwe, E. Vittoz, and I. Verbauwhede, "A micropower CMOS-instrumentation amplifier," *IEEE J. Solid-State Circuits*, vol. SC-20, pp. 805–807, June 1985.

[13] C. G. Yu and R. L. Geiger, "Precision offset compensated op-amp with ping-pong control," in *GOMAC-92 Dig.*, 1992.

Chong-Gun Yu received the B.S. and M.S. degrees in electronic engineering from Yonsei University, Seoul, Korea, in 1985 and 1987, respectively.

He was a graduate student at Texas A&M University, College Station, from 1989 to 1990. In 1991 he transferred to Iowa State University, Ames, where he is currently working toward the Ph.D. degree. His research interests include high-precision analog circuit design, continuous-time filter design and tuning, system identification, and mixed-signal IC design.

Randall L. Geiger (S'75–M'77–SM'82–F'90) received the B.S. degree in electrical engineering and the M.S. degree in mathematics from the University of Nebraska in 1972 and 1973, respectively, and the Ph.D. degree in electrical engineering from Colorado State University in 1977.

He was a faculty member at Texas A&M University from 1977 to 1990. He joined the Electrical Engineering and Computer Engineering Department at Iowa State University in 1991, and currently serves as Professor and Chairman in the Department.

Dr. Geiger is a past Associate Editor of the IEEE TRANSACTIONS ON CIRCUITS AND SYSTEMS and a past Circuits and Systems Society Editor of the *Circuits and Devices Magazine*. He is currently serving on the IEEE Periodicals Council, the IEEE Publications Board, and as President of the Circuits and Systems Society.